Solar Phys (2011) 274:285–301
DOI 10.1007/s11207-010-9657-6

The Floor in the Solar Wind Magnetic Field Revisited

E.W. Cliver · A.G. Ling

Received: 30 August 2010 / Accepted: 14 October 2010 / Published online: 10 November 2010

Abstract Svalgaard and Cliver (*Astrophys. J. Lett.* **661**, L203, 2007) proposed that the solar-wind magnetic-field strength [B] at Earth has a "floor" value of ≈ 4.6 nT in yearly averages, which is approached but not broached at solar minima. They attributed the floor to a constant baseline solar open flux. In both 2008 and 2009, the notion of such a floor was undercut by annual B averages of ≈ 4 nT. Here we present a revised view of both the level and the concept of the floor. Two independent correlations indicate that B has a floor of ≈ 2.8 nT in yearly averages. These are *i*) a relationship between solar polar-field strength and yearly averages of B for the last four 11-year minima ($B_{\rm MIN}$), and *ii*) a precursor relationship between peak sunspot number for cycles 14 – 23 and $B_{\rm MIN}$ at their preceding minima. These correlations suggest that at 11-year minima, B consists of *i*) a floor of ≈ 2.8 nT, and *ii*) a component primarily due to the solar polar fields that varies from ≈ 0 nT to ≈ 3 nT. The solar polar fields provide the "seed" for the subsequent sunspot maximum. Removing the ≈ 2.8 nT floor from $B_{\rm MIN}$ brings the percentage decrease in B between the 1996 and 2009 minima into agreement with the corresponding decrease in solar polar-field strength. Based on a decomposition of the solar wind (from 1972 – 2009) into high-speed streams, coronal mass ejections, and slow solar wind, we suggest that the source of the floor in B is the slow solar wind. During 2009, Earth was in slow solar-wind flows $\approx 70\%$ of the time. We propose that the floor corresponds to a baseline (non-cyclic or ground state) open solar flux of $\approx 8 \times 10^{13}$ Wb, which originates in persistent small-scale (supergranular and granular) field.

Keywords Solar wind · Slow solar wind · Floor · Cycle 24

The Sun – Earth Connection near Solar Minimum
Guest Editors: M.M. Bisi, B.A. Emery, and B.J. Thompson

E.W. Cliver (✉)
Space Vehicles Directorate, Air Force Research Laboratory, Hanscom AFB, MA, USA
e-mail: afrl.rvb.pa@hanscom.af.mil

A.G. Ling
Atmospheric Environmental Research, Inc., Lexington, MA, USA

1. Introduction

Svalgaard and Cliver (2007) proposed that the solar-wind magnetic-field magnitude [B] had a floor of ≈ 4.6 nT in yearly averages, a value which the interplanetary magnetic-field [IMF] strength returned to, or approached, at each solar minimum from 1872 – 2004. For solar cycles prior to the space age, annual averages of B were inferred from the interdiurnal variability (IDV) index of geomagnetic activity (Svalgaard and Cliver, 2005). This empirical/historical evidence for a lower limit or floor in B was substantiated by Carrington-rotation averages of direct measurements of B since 1965 and by measurements of cosmogenic nuclei in ice cores and tree rings since 1500, scaled to the B-series derived from IDV (Svalgaard and Cliver, 2007, and references therein). The notion of a floor in solar wind B is consistent with the model of Fisk and Schwadron (2001) for the reversal of the polar magnetic fields at solar maximum. The Fisk and Schwadron model, based on the interchange reconnection process (Crooker, Gosling, and Kahler, 2002), postulates the constancy of the solar open flux. The existence of a floor is implicit in the work of Owens and Crooker (2006, 2007) who simulated the interplanetary magnetic-field strength in terms of a constant open-flux component and a superposed 11-year time-varying contribution from coronal mass ejections (CMEs).

The proposed ≈ 4.6 nT floor in B was short-lived. For 2009, the average of B was 3.93 nT. This observation has prompted a major revision in the level of the floor, as well as the view of its origin, which is presented in this paper.

The revised picture is based on two correlations. Both of these correlations involve the solar polar fields and taken together they point to a level of the floor significantly lower than the originally proposed ≈ 4.6 nT.

The first of these correlations is a precursor relationship (Schatten *et al.*, 1978) in which the measured solar poloidal field (the dipole moment [DM]), or a proxy, at solar minimum serves as an indicator of the strength of the toroidal magnetic field (peak sunspot number [SSN_{MAX}]) at the subsequent sunspot maximum. Quoting from Schatten *et al.* (1978): " ... it is the polar flux, wound by differential rotation into a subsurface toroidal flux, which emerges as the next cycle's sunspots. Thus, on physical grounds, we believe the strength of the sun's polar magnetic field at minimum is related to the next cycle's sunspot activity." From the precursor relationship between SSN_{MAX} and DM, Svalgaard, Cliver, and Kamide (2005) predicted that the peak sunspot number of Cycle 24 would be 75 ± 8, near the value of 90 recently adopted by the NOAA/NASA/ISES prediction panel (http://www.swpc.noaa.gov/SolarCycle/SC24/index.html). The Svalgaard *et al.* prediction was based on measurements of DM at the minima preceding Cycles 22 (1986) and 23 (1996) and the assumption that zero polar-field strength corresponded to zero SSN_{MAX}. Because of the importance of the prediction of SSN_{MAX} for technology operators/planners affected by the space environment, it would be useful to substantiate this forecast for the peak of cycle 24, which is predicted to occur in May 2013. We will do that in this study, but the main purpose here is to revisit the concept of the floor.

In addition to determining the peak sunspot number of the approaching cycle, the solar polar fields at 11-year minima are thought, following Pneuman and Kopp (1971) and Schatten (1971), to be the principal source of the solar wind near Earth during solar minima. It was surprising then that long-term reconstructions of the solar wind (Svalgaard and Cliver, 2005) showed that at solar minimum for the last 12 cycles, annual averages of B [B_{MIN}] only varied between 4.7 – 6.0 nT, during which time cycles with peak SSNs as high as 201.3 (Cycle 19) and as low as 64.2 (Cycle 14) were observed. This suggested that either the precursor technique was not valid or that B_{MIN} must be, at best, only weakly dependent on the

polar fields. *Ulysses* observations of the radial solar-wind magnetic field [B_R] suggested the latter. B_R was reported to be constant at $\approx 3.2 \pm 0.3$ nT near the two minima flanking cycle 23 (Balogh and Smith, 2006) for which the measured polar fields strengths were ≈ 200 μT and ≈ 120 μT, respectively. Thus, Svalgaard and Cliver (2007) proposed a "floor" in yearly averages of the solar-wind magnetic-field strength [B] of ≈ 4.6 nT that was independent of DM. They equated the floor with a constant radial component of the solar magnetic field [B_R] of ≈ 3 nT corresponding to a baseline solar magnetic flux of $\approx 4 \times 10^{14}$ Wb.

The floor in B_R of ≈ 3 nT at *Ulysses* was undercut by new observations. Smith and Balogh (2008) reported that B_R dropped to ≈ 2.3 nT during the *Ulysses* fast-latitude scan in 2006 – 2007, from a recalculated value of 3.6 nT near the 1994 – 1995 fast scan. As noted above, the average value of B at Earth dropped to 3.93 nT during 2009, following values of 4.48 nT in 2007 and 4.21 nT in 2008. Clearly B_{MIN} was responding to the change in the polar fields. This introduces the second correlation on which the revised view of the floor is based – a relationship between B_{MIN} and DM.

In this study, we determine the relationship between B_{MIN} and DM and obtain a precursor relationship for SSN_{MAX} based on B_{MIN}. These two relationships independently point to a floor value of ≈ 2.8 nT. We then use *in-situ* solar-wind observations since 1972, and particularly from the current deep 11-year minimum, to gain insight concerning the source of such a floor. Our analysis is presented in Section 2 and our findings are summarized and discussed in Section 3.

2. Analysis

2.1. Data

Tables 1 and 2 contain the data used in this study.

Table 1 lists the yearly sunspot number, the percentage of time per year that solar-wind observations were available, and annual averages of solar wind V, B, and B_R (from the NASA/OMNI data base) for the years 1965 – 2009. The open solar flux [Φ] at 1 AU given for each year is calculated from the following relationship:

$$\Phi(\mathrm{Wb}) = 1/2\left[4\pi R^2 B_R\right], \tag{1}$$

based on the "*Ulysses* result" (Balogh *et al.*, 1995; Smith and Balogh, 1995; Lockwood *et al.*, 2004; Lockwood and Owens, 2009) that B_R (normalized to 1 AU) is independent of latitude with an uncertainty of $< 5\%$ when averaged over time periods of a solar rotation or more, allowing Φ to be determined from single-point measurements of B_R. In Equation (1), the factor of one-half reflects the fact that half the Sun's open flux is directed inward and the other half outward. For observations at 1 AU, $R = 1.5 \times 10^{13}$ cm. The listed annual average of B_R was determined by first summing signed hourly values of B_R over a day (for days with at least 12 hours of observations) and then dividing the absolute value of the sum by the number of hourly observations in a day. As shown by Lockwood *et al.* (2006), pre-averaging B_R over a day brings the magnetic flux measured *in-situ* at Earth into agreement with that determined from solar magnetograph data and the potential-field source-surface model (Wang and Sheeley, 1995, 2002). This simple pre-averaging technique gives results in reasonably good agreement with a more detailed kinematic correction recently developed by Lockwood, Rouillard, and Finch (2009) and Lockwood, Owens, and Rouillard (2009a, 2009b), which makes allowance for the effect of longitudinal structure in the solar-wind flow speed.

Table 1 Sunspot numbers and solar wind parameters (1965 – 2009).

Year	SSN	SW Cov. [%]	V [km s^{-1}]	B [nT]	B_R [nT]	Φ 10^{14} [Wb]	Time (HSS) [%]	Time (SSW) [%]	Time (CME) [%]	B_{UNC} [nT]	B_{HSS}[a] [nT]	B_{SSW}[a] [nT]	B_{CME}[a] [nT]	$\langle V_{SSW} \rangle$ [km s^{-1}]	$\langle B_{SSW} \rangle$ [nT]
1965	15.1	43	420	5.06	1.86	2.62	–	–	–	–	–	–	–	–	–
1966	47.0	34	430	6.35	2.54	3.59	–	–	–	–	–	–	–	–	–
1967	93.8	80	428	6.36	2.41	3.41	–	–	–	–	–	–	–	–	–
1968	105.9	63	468	6.19	2.44	3.44	–	–	–	–	–	–	–	–	–
1969	105.5	69	420	6.05	2.41	3.41	–	–	–	–	–	–	–	–	–
1970	104.5	61	422	6.35	2.46	3.48	–	–	–	–	–	–	–	–	–
1971	66.6	40	441	6.00	2.19	3.09	–	–	–	–	–	–	–	–	–
1972	68.9	46	403	6.38	2.38	3.36	36.1	40.9	23.0	1.69	2.33	2.30	1.76	359	5.35
1973	38.0	73	485	6.35	2.85	4.03	58.8	31.4	9.8	0.23	4.05	1.58	0.71	373	5.19
1974	34.5	94	525	6.63	3.00	4.23	70.1	22.8	7.1	0.22	4.64	1.30	0.69	391	5.82
1975	15.5	76	486	5.82	2.47	3.50	61.0	31.9	7.2	0.22	3.66	1.63	0.53	372	4.98
1976	12.6	70	445	5.45	2.36	3.34	50.8	43.7	5.5	0.11	2.83	2.30	0.32	374	4.86
1977	27.5	86	413	5.85	2.24	3.16	50.2	36.0	13.8	–	3.00	1.97	0.88	352	5.26
1978	92.5	82	428	7.08	2.53	3.58	32.8	37.9	29.2	0.09	2.26	2.15	2.68	354	5.82
1979	155.1	91	417	7.59	3.14	4.44	35.3	35.9	28.8	0.01	2.61	2.40	2.58	355	6.73
1980	154.6	92	391	6.98	2.52	3.57	33.3	30.8	35.9	0.30	2.27	1.84	2.88	332	6.07
1981	140.5	91	425	7.84	3.06	4.32	28.4	29.5	42.0	0.11	2.17	1.89	3.78	362	6.44
1982	115.9	69	467	8.81	3.79	5.36	47.0	23.1	29.9	1.15	3.80	1.64	3.37	374	7.66
1983	66.8	36	473	7.94	3.35	4.74	57.4	28.3	14.3	0.27	4.58	2.09	1.26	398	7.07
1984	45.7	26	476	7.88	3.93	5.55	59.8	34.3	5.9	0.56	4.19	3.05	0.64	394	7.31
1985	17.9	32	466	5.89	2.60	3.67	51.4	39.9	8.7	1.10	3.20	2.10	0.59	369	5.20
1986	13.4	42	453	5.74	2.42	3.42	45.4	45.1	9.5	0.10	2.44	2.67	0.63	377	5.11
1987	29.5	43	429	6.09	2.47	3.49	51.9	39.5	8.6	0.09	3.06	2.53	0.49	360	5.51
1988	100.2	43	429	7.30	3.01	4.26	41.7	36.0	22.3	0.47	2.73	2.78	1.79	358	6.54

Table 1 (*Continued.*)

Year	SSN	SW Cov. [%]	V [km s^{-1}]	B [nT]	B_R [nT]	Φ 10^{14} [Wb]	Time (HSS) [%]	Time (SSW) [%]	Time (CME) [%]	B_{UNC} [nT]	B_{HSS}[a] [nT]	B_{SSW}[a] [nT]	B_{CME}[a] [nT]	$\langle V_{SSW} \rangle$ [km s^{-1}]	$\langle B_{SSW} \rangle$ [nT]
1989	157.6	44	451	8.15	3.43	4.85	15.4	28.4	56.2	0.32	1.38	2.64	4.14	372	7.26
1990	142.5	41	445	7.29	3.36	4.75	31.0	29.8	39.2	0.51	2.22	2.16	2.91	373	6.49
1991	145.7	40	463	9.34	4.03	5.69	29.7	23.2	47.1	0.32	2.64	2.39	4.31	359	8.10
1992	94.3	38	430	8.25	3.25	4.60	33.8	37.6	28.6	0.28	2.45	2.80	3.00	368	6.69
1993	54.6	33	448	6.59	2.98	4.21	60.8	34.4	4.8	0.35	3.88	2.47	0.24	359	6.00
1994	29.9	42	527	6.15	2.69	3.80	67.3	28.4	4.3	0.06	4.28	1.60	0.27	375	5.54
1995	17.5	97	429	5.73	2.20	3.11	44.5	51.8	3.6	–	2.82	2.55	0.36	353	4.92
1996	8.8	94	424	5.11	2.06	2.91	57.3	41.2	1.5	0.05	3.06	1.91	0.13	363	4.57
1997	21.5	91	381	5.54	1.93	2.73	32.0	54.4	13.6	0.00	1.79	2.50	1.25	340	4.62
1998	64.3	100	411	6.89	2.55	3.60	31.4	41.7	26.8	0.11	2.15	2.39	2.35	364	5.72
1999	93.3	100	438	6.91	2.74	3.87	42.3	37.1	20.6	0.10	2.99	2.28	1.63	371	6.12
2000	119.6	100	447	7.18	2.70	3.81	29.3	33.5	37.2	0.02	1.94	2.03	3.21	367	6.06
2001	111.0	100	425	6.94	2.52	3.57	29.0	35.2	35.8	0.12	2.04	1.96	2.93	357	5.55
2002	104.1	100	439	7.64	3.31	4.68	49.9	28.8	21.3	0.16	3.77	1.87	2.00	355	6.49
2003	63.7	99	541	7.60	3.60	5.09	64.6	20.6	14.7	–	4.78	1.33	1.48	405	6.45
2004	40.4	100	451	6.53	2.84	4.02	41.7	46.3	12.0	–	2.77	2.55	1.21	380	5.51
2005	29.8	99	468	6.25	2.61	3.68	41.4	38.3	20.3	–	2.54	2.05	1.66	366	5.36
2006	15.2	100	429	5.03	1.89	2.67	43.0	50.5	6.4	–	2.22	2.28	0.53	349	4.50
2007	7.6	100	440	4.48	1.67	2.35	54.0	45.5	0.6	–	2.58	1.83	0.07	344	4.03
2008	2.8	99	450	4.21	1.67	2.35	55.0	44.0	1.0	–	2.55	1.60	0.06	346	3.67
2009	3.1	100	364	3.93	1.25	1.77	25.1	71.3	3.6	–	1.10	2.60	0.23	336	3.65

[a]The contributions from the unclear category have been apportioned to the three basic flow types according to the amount of time Earth spent in each type (T_{HSS}, T_{SSW}, T_{CME}) so $B_{HSS} + B_{SSW} + B_{CME} = B$. The sum of $T_{HSS} + T_{SSW} + T_{CME}$ was normalized to 100% for the apportionment process.

Table 2 Data for precursor predictions of SSN(Max).

SSN[a] Min Year (Cycle)	SSN Min	SSN Max (Year)	$\langle B \rangle$ [nT]	DM [μT]
1901 (14)	3.2	77.0 (1906)	4.06	–
1913 (15)	1.7	126.5 (1917)	4.18	–
1923 (16)	7.0	93.7 (1928)	4.70	–
1934 (17)	10.4	143.0 (1937)	5.02	–
1944 (18)	11.5	151.8 (1947)	5.71	–
1954 (19)	4.4	201.3 (1958)	5.32	–
1965 (20)	15.1	110.6 (1968)	5.06	–
1976 (21)	12.6	164.5 (1979)	5.45	240
1986 (22)	13.4	158.5 (1989)	5.74	250
1996 (23)	8.8	120.8 (2000)	5.11	199
2009 (24)	3.1	[64.7] [2013]	3.93	107

[a]See text.

Table 1 also includes the contributions to annual averages of IMF strength by the three components of the solar wind [high-speed streams (HSSs), slow solar wind (SSW), and coronal mass ejections (CMEs)] for the years 1972 – 2009 (Richardson, Cliver, and Cane, 2000; Richardson, Cane, and Cliver, 2002; Richardson, personal communication, 2010). As discussed in Richardson, Cliver, and Cane (2000), the separation of the solar wind into HSSs, SSW, and CMEs is based on the *in-situ* signatures of these flow types, *e.g.* low proton temperature, magnetic clouds, bi-directional particle streaming, Forbush decreases, and helium abundance enhancements for CMEs. For a small fraction of time, the classification was indeterminate. Note that the contributions of each flow type to the annual average of B, designated by B_{HSS}, B_{SSW}, and B_{CME} in Table 1, are not the average B in each flow type, although the sum of the three contributions adds up to average B for each year. Rather it is what the average B would have been for a given flow type in the absence of the other two types and the unclassified [designated B_{UNC}] flows (setting their contributions equal to zero and dividing the sum of hourly average B values, *e.g.* $\sum B_{\mathrm{CME}(i)}$, by the total number of hours of observations during a given year ($T_{\mathrm{OBS}} = T_{\mathrm{HSS}} + T_{\mathrm{SSW}} + T_{\mathrm{CME}} + T_{\mathrm{UNC}}$)), *i.e.*

$$\langle B \rangle = \sum B_{\mathrm{HSS}(i)}/T_{\mathrm{OBS}} + \sum B_{\mathrm{SSW}(i)}/T_{\mathrm{OBS}} + \sum B_{\mathrm{CME}(i)}/T_{\mathrm{OBS}} + \sum B_{\mathrm{UNC}(i)}/T_{\mathrm{OBS}}, \quad (2)$$

where $\langle B \rangle$ = the annual average of B. In Table 1, the contribution to $\langle B \rangle$ from the unclassified solar-wind intervals has been apportioned to the contributions from the other three flow

Table 3 Relationship between minimum-to-minimum changes in the solar polar-field strength (DM) and the solar wind field strength (B).

Cycles	ΔDM	ΔB_{MIN} (without floor subtraction)	ΔB_{MIN} (with floor subtraction)
21 – 22	+4%	+5%	+11%
22 – 23	−20%	−11%	−21%
23 – 24	−46%	−23%	−51%

types (B_{HSS}, B_{SSW}, B_{CME}) based on the listed percentage of time that Earth spent in each of these flows during the year (T_{HSS}, T_{SSW}, T_{CME}). The last two columns in the table give annual averages of $B(\langle B\rangle)$ and $V(\langle V\rangle)$ for the slow solar wind.

Table 2 gives B_{MIN} for the 11-year magnetic minima preceding Cycles 14 – 23 and SSN_{MAX} for their associated maxima. Generally, years of magnetic minima correspond to solar minima. For three of the solar cycles in Table 2 [17, 20, and 24], however, the magnetic minimum followed the sunspot minimum by a year. The B_{MIN} values beginning with 1965 were obtained from the OMNI data base. For earlier minima, B_{MIN} values are based on the interdiurnal variability [IDV] index of geomagnetic activity (Svalgaard and Cliver, 2005, 2010). DM, for minima preceding cycles 22 – 24, is the absolute value of the difference (in μT) between the north and south polar field magnitudes as measured at Wilcox Solar Observatory (WSO; Svalgaard, Cliver, and Kamide, 2005). The listed values are averages obtained for the three-year periods ending with the year of magnetic minimum. Svalgaard and Schatten (2008) reanalyzed and reconciled discordant solar magnetic-field data from WSO and Mount Wilson Observatory to obtain the DM value for Cycle 21. The listed maximum sunspot numbers are peak values smoothed over a 13-month period. The SSN_{MIN} values are yearly averages. For years prior to 1947, both the SSN_{MAX} and SSN_{MIN} values have been adjusted upward by 20% to correct for the "Waldmeier discontinuity" (Svalgaard, 2010). This discontinuity is an upward offset in the international sunspot number that occurred shortly after Waldmeier took over the production of the Zürich SSN from Brunner.

2.2. Correlation between Solar Wind B and Solar Polar Magnetic-field Strength at Solar Minimum

Following Pneuman and Kopp (1971) and Schatten (1971), we might expect that the minimum-to-minimum change in solar wind B (*i.e.* B_{MIN}) values would be directly proportional to the corresponding change in the solar polar-field strength. In Figure 1, however, the relationship between B_{MIN} and DM for Cycles 21 – 24, does not pass through the origin. The intercept of 2.63 nT, based on a linear extrapolation of the relationship given in the figure to DM = 0, implies that when/if the solar polar fields disappear, the magnetized solar wind persists. We suggest that this persistent field constitutes the floor in the solar-wind magnetic-field strength.

Figure 1 shows that the 46% decrease in DM between the minima preceding Cycles 23 and 24 (from 199 μT to 107 μT) was accompanied by a 23% reduction in B_{MIN} (from 5.11 nT to 3.93 nT). An approximate proportionality between the changes at the Sun and Earth is achieved if one measures B_{MIN} above the ≈ 2.8 nT floor; then we have a 51% $[(2.31 - 1.13)/2.31]$ decrease in B_{MIN}. Table 3 shows that this approximate proportionality between changes in DM and changes in B_{MIN} (measured above the floor) also holds for the minimum-to-minimum changes between Cycles 21 and 22 and Cycles 22 and 23.

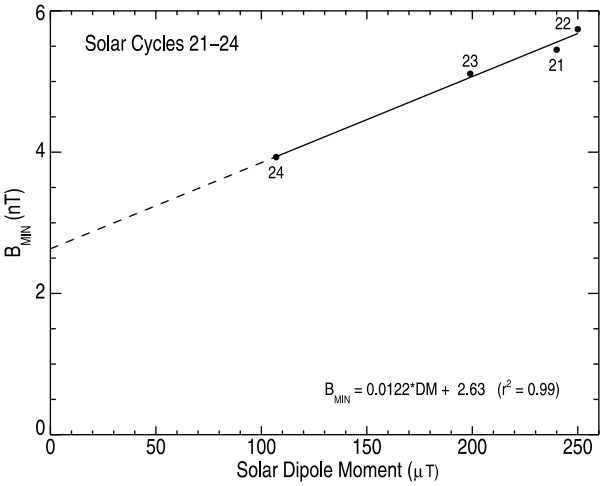

Figure 1 Solar magnetic-field strength [$B_{\rm MIN}$] at the last four solar minima (Cycles 21 – 24) plotted *vs*. the solar dipole-field strength [DM], with (geometric mean) regression line.

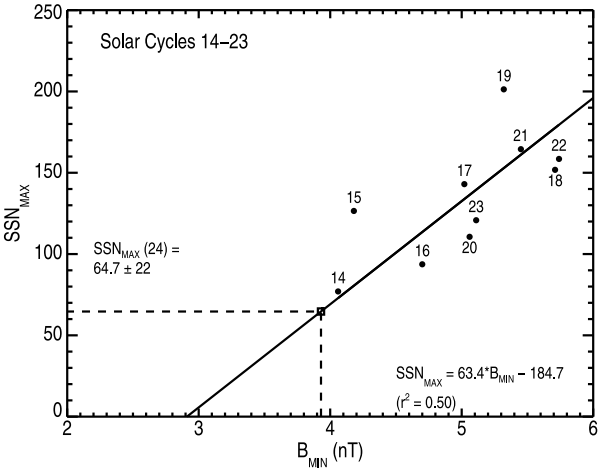

Figure 2 The peak sunspot number [$\rm SSN_{MAX}$] of Solar Cycles 14 – 23 plotted *vs*. the observed or inferred solar-wind magnetic-field strength at the preceding minimum [$B_{\rm MIN}$], with (geometric mean) regression line.

2.3. Precursor Relationship between $\rm SSN_{MAX}$ and $B_{\rm MIN}$

The correlation in Figure 1 supports the use of $B_{\rm MIN}$ in a precursor relationship to predict the next solar cycle (*cf*. Wang and Sheeley, 2009). It enables us to check the $\rm SSN_{MAX}$ prediction of Svalgaard, Cliver, and Kamide (2005) for Cycle 24 that was based on only two cycles of measured solar polar fields with a precursor relationship based on ten cycles of measured and inferred $B_{\rm MIN}$ values. A scatter plot of $\rm SSN_{MAX}$ *vs*. $B_{\rm MIN}$ at the preceding minimum for Solar Cycles 14 – 23 is given in Figure 2. The least-square line through these points yields a prediction of 64.7 for the $\rm SSN_{MAX}$ of Cycle 24 ($B_{\rm MIN} = 3.93$ nT), with a statistical error bar (simple average of the unsigned error for Cycles 14 – 23) of ± 22.[1] Note that a predicted

[1]There is a caveat that applies to this $\rm SSN_{MAX}$ prediction and all others for Cycle 24. Penn and Livingston (2006) reported a 52 G year^{-1} decrease in the maximum magnetic fields of sunspots from 1998 – 2005. If this decrease continues (see Livingston and Penn, 2009), the predicted number of sunspots in Cycle 24 will be reduced by $\approx 50\%$.

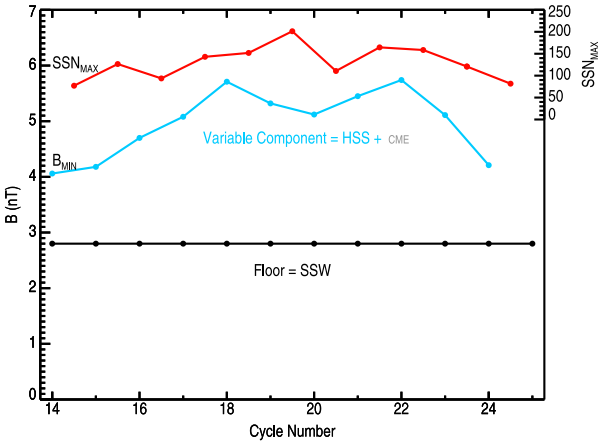

Figure 3 Our conception of the solar wind magnetic-field strength [B] at minimum, shown for Cycles 14 – 24. At 11-year minima, we propose that B consists of a ≈ 2.8 nT floor attributed to the slow solar wind, and a variable component ($\lesssim 3$ nT) due primarily to high-speed streams from polar coronal holes (with a small/negligible contribution from CMEs) that provides the seed field for the next solar maximum. The peak sunspot numbers for the maxima following each minimum are shown at the top of the figure. The $\mathrm{SSN_{MAX}}$ values are plotted one-half cycle after their preceding minima.

$\mathrm{SSN_{MAX}}$ of 0 corresponds to $B_{\mathrm{MIN}} = 2.91$ nT, in reasonable agreement with the 2.63 nT intercept in Figure 1. Because of the uncertainties involved, we take the floor in B to be ≈ 2.8 nT, the approximate average of 2.63 nT and 2.91 nT.

2.4. The Solar Wind at 11-year Minima and the Source of the Floor

The two correlations discussed in the preceding sections suggest that at solar minimum, solar-wind B consists primarily of *i*) a ≈ 2.8 nT floor, and *ii*) a component ranging from ≈ 0 nT to ≈ 3 nT that varies from cycle to cycle in concert with the solar polar fields. For years of solar minima, CMEs make a relatively small contribution to B and low-latitude coronal holes are largely absent (Wang and Sheeley, 1994).[2] Thus, it is natural to attribute the variable component that rides atop the floor primarily to the polar coronal holes and their associated HSSs, leaving the SSW as the putative source of the floor. Figure 3 shows the separation of solar wind B at the minima of Cycles 14 – 24 into these two components (where the contributions from the polar holes and CMEs have been combined) along with the envelope of $\mathrm{SSN_{MAX}}$ values over the same period. The variable component of B_{MIN} that lies above the floor mimics the variation of the envelope of peak 11-year sunspot numbers over the 20$^{\mathrm{th}}$ century. It shows the general rise in $\mathrm{SSN_{MAX}}$ values from small Cycle 14 to the large Cycles 18 and 19 at mid-century, which were followed in turn by low Cycle 20, large Cycles 21 and 22, and the descent into what appears to be a coming Gleissberg-type (if not Maunder-type) minimum.

Table 4, based on a subset of data from Table 1, provides support for the conjecture that SSW is the source of the floor. The first row in this table gives values of the following parameters for the three solar minima preceding Cycles 21, 22, and 23: average B, the

[2]For all but one of the 11 minima in Table 2, $B_{\mathrm{CME}} \lesssim 0.3$ nT, based on direct observations for Cycles 21 – 24 and a correlation between yearly sunspot number and B_{CME} for the seven earlier minima in Table 2. For 1986, $B_{\mathrm{CME}} = 0.63$ nT.

Table 4 Solar and solar-wind parameters for recent levels of B_{MIN}, with extrapolation to the floor.

Min. Year(s)	B_{MIN} [nT]	SSW [% Time]	SSW $\langle B \rangle$	SSW $\langle V \rangle$
⟨1976, 1986, 1996⟩	5.43 nT	43.3%	4.85 nT	372 km s^{-1}
2009	3.93 nT	71.3%	3.65 nT	336 km s^{-1}
Floor	$\approx$ 2.8 nT	(92%)	(2.75 nT)	(309 km s^{-1})

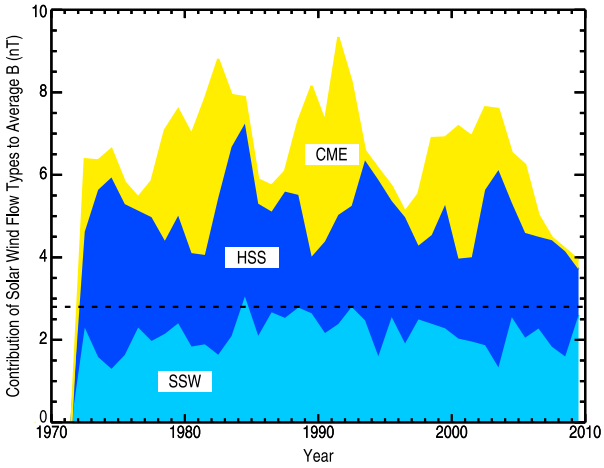

Figure 4 Cumulative distribution of the contribution of SSW, HSSs, and CMEs to average B from 1972 – 2009. The dashed line is drawn at the floor value of $\approx$ 2.8 nT.

percentage of time Earth spent in slow solar-wind flows (normalized to 100% classification), and average B and V for the SSW. The second row gives values of these parameters for 2009, the magnetic minimum of Cycle 24. Note the sharp increase in the percentage of time Earth spent in SSW (primarily at the expense of HSSs) between the 1976/1986/1996 minima and 2009. A drop of 1.50 nT in the average B_{MIN} from Cycles 21/22/23 (5.43 nT) to Cycle 24 (3.93 nT) was accompanied by an increase of 28% (from 43% to 71%) in the amount of time Earth spent in SSW. Extrapolating another 1.13 nT to the $\approx$ 2.8 nT floor, and assuming that the percentage of time in SSW changes proportionately, *i.e.*

$$X/(2.63\ \text{nT}) = 28\%/(1.50\ \text{nT}), \tag{3}$$

where $X + 43\% = \%$ of time Earth spends in the slow solar wind when $B \approx 2.8$ nT, indicate that Earth would be in SSW 92% of the time at floor conditions (row three). Moreover, making the same assumption for average B in the slow solar wind indicates that this parameter would drop to 2.75 nT, near the $\approx$ 2.8 nT floor. A similar extrapolation for V yields 309 km s^{-1}. Insofar as the current solar minimum provides the best observed "glimpse" of the floor in the solar wind that we have had to date, Table 4 strongly suggests that the slow solar wind is the source of the floor.

The floor-like quality of the SSW can be seen in the cumulative distribution graph in Figure 4, which shows the contribution, from Table 1, of each of the three flow types to the average B for 1972 – 2009. The average contribution of SSW to B during this period [B_{SSW}] was 2.16 nT, with a standard deviation of 0.42 nT. The SSW contribution is relatively constant. In particular, there is no apparent 11-year variation. The fact that the average value of B_{SSW} lies below the floor value of $\approx$ 2.8 nT likely reflects the separation of the three components according to their geomagnetic impact (Richardson, Cliver, and Cane, 2000).

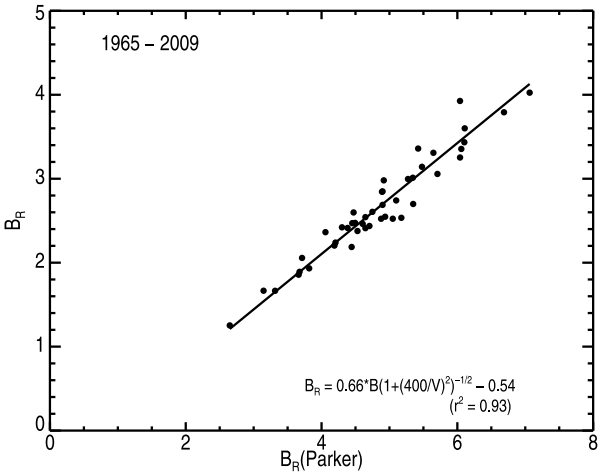

Figure 5 Scatter plot of observed B_{R} *vs.* the theoretical B_{R}, designated B_{R}(Parker), from 1965 – 2009 with (geometric mean) regression line.

Thus SSW in co-rotating active regions and at shock fronts is attributed to HSSs and CMEs, respectively, reducing the contribution of SSW to B. When Earth is in slow flows for a large percentage of time during the year, we would expect the "loss" of B_{SSW} to these other components to diminish and B_{SSW} to approach the floor value of ≈ 2.8 nT, as it did in 2009 when $B_{\mathrm{SSW}} = 2.60$ nT. The 71% of the time that Earth was in slow flows during 2009 was exceptional. Only for three prior years did the SSW percentage exceed 50% and the average B_{SSW} for these years was 2.44 nT [1995 (52%, $B_{\mathrm{SSW}} = 2.55$ nT), 1997 (54%, 2.50 nT), and 2006 (51%; 2.28 nT)].

Ultimately, in the picture that we are proposing, the average B during floor conditions is determined by the fixed amount of open flux associated with the slow solar wind. To determine Φ from B, we need to take into account the dependence of B_{R} on V in accord with Parker spiral theory (Rouillard, Lockwood, and Finch, 2007). Figure 5 gives a scatter plot of observed B_{R} *vs.* the theoretical B_{R}, designated B_{R}(Parker), from 1965 – 2009, where

$$B_{\mathrm{R}}(\mathrm{Parker}) = B\left[1 + (r\omega \cos\psi / V)^2\right]^{-1/2} \tag{4}$$

and $r = 1$ AU, ω is the Sun's angular velocity, and ψ is the heliographic latitude of the Earth. The resultant simplified regression equation given in Figure 5 is nearly identical to that obtained by Rouillard, Lockwood, and Finch (2007) for the years 1967 – 2004. Inserting floor values of $B = 2.8$ nT and $V = 300$ km s^{-1} in this equation yields $B_{\mathrm{R}} = 0.57$ nT. Then Equation (1) yields a floor value for Φ of $\approx 8 \times 10^{13}$ Wb, a value considerably lower than the $\approx 4 \times 10^{14}$ Wb given in Svalgaard and Cliver (2007). The decrease in Φ is due to the decrease in the floor value of B, and also to the one-day pre-averaging of B_{R} and the allowance for velocity dependence, neither of which were considered in the original estimate.

The eclipse image taken on 22 July 2009 (Figure 6(a)) indicates that as the floor in B is approached, the slow solar wind extends to relatively high latitudes. This image and one taken during the comparable minimum year of 1901 (Figure 6(b)) show closed loops near the poles. During the Maunder Minimum (MM, 1645 – 1715; Eddy, 1976), the polar fields would have been weaker, if not absent, and the polar holes were presumably even more

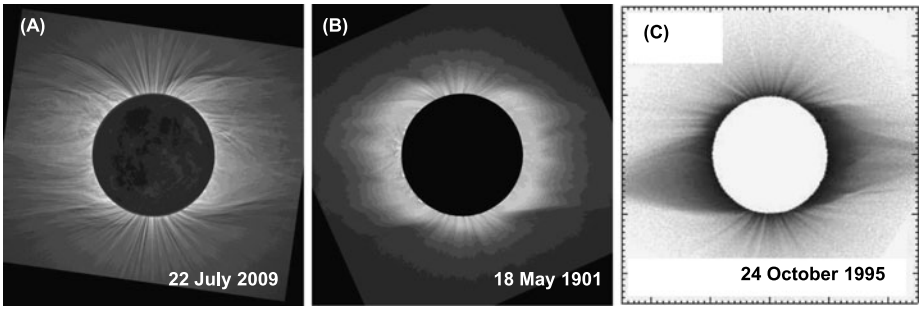

Figure 6 The solar corona on: (a) 22 July 2009, (b) 18 May 1901, and (c) 24 October 1995. The corona in (c) represents a classic case in which the streamer belt is confined near the solar equatorial plane. In the non-canonical minimum coronae in (a) and (b), the streamer belt is much thicker in appearance. The images in (a) and (b) are from the eclipse archive of the High Altitude Observatory (http://mlso.hao.ucar.edu/mlso_eclipses.html). The eclipse photograph in (c) was taken from Judge *et al.* (2010); the image was obtained by Rušin and processed by Druckmüller.

constricted by such arcades.[3] In contrast to the coronas depicted in Figures 6(a, b), the solar polar fields during the more "canonical" solar minimum eclipse on 24 October 1995 were strong and the streamer belt was close to the solar equatorial plane (Figure 6(c)). While the average tilt angle of the heliospheric current sheet was low (average value $\approx 20°$) during 2009, consistent with relatively little large-scale warp, coronal complexity clearly extended to high latitudes. Judge *et al.* (2010) attribute the complex structure of the corona in 1901 and 2009 to higher-order multipolar structure, associated with high-latitude prominence cavities.

3. Conclusion

3.1. Summary

We obtained a relationship between the solar-wind magnetic-field strength [$B_{\rm MIN}$] and the solar polar field strength [DM] for the last four solar minima (Figure 1). The apparent close correlation between these parameters justified the construction of a precursor relationship for $\rm SSN_{MAX}$ using $B_{\rm MIN}$ as the independent or driving variable. This precursor relationship was based on ten cycles of $B_{\rm MIN}$ data (four for which $\rm B_{MIN}$ was directly observed, and six for which it was obtained from geomagnetic-based reconstructions). We used this relationship and the $B_{\rm MIN}$ value for 2009 to predict a peak sunspot number of 65 ± 22 for Cycle 24 (Figure 2), consistent with the earlier prediction of 75 ± 8 of Svalgaard, Cliver, and Kamide (2005), which was based on only two cycles of polar field data and a forced fit through the origin. Both the $B_{\rm MIN} vs.$ DM and $\rm SSN_{MAX}$ *vs.* $B_{\rm MIN}$ relationships indicate the existence of a floor in the solar-wind magnetic-field strength of ≈ 2.8 nT for a DM at solar minimum of ≈ 0 μT. In other words, when the solar polar fields approach zero at the minima preceding

[3]It is doubtful that the polar fields and solar cycle disappeared during the MM. Sunspots were reported sporadically at low levels throughout this period (see, *e.g.*, Eddy, 1976; Hoyt and Schatten, 1998) and evidence from the ^{10}Be concentration in ice cores indicates that the 11-year cycle continued during the MM (Beer, Tobias, and Weiss, 1998; Berggren *et al.*, 2009). Recently, however, Webber, Higbie, and Webber (2010) have challenged the ^{10}Be-based reconstructions of B. These authors suggest that "more than 50% of the ^{10}Be flux increase around, *e.g.*, 1700 AD, 1810 AD and 1895 AD is due to non-production related increases".

weak cycles, such as those of the Maunder Minimum, there will still be a magnetized solar wind. The existence of such a floor brings cycle-to-cycle changes in $B_{\rm MIN}$ (measured above the floor) and DM into approximate proportionality (Table 3). We suggest that at solar minimum, the solar-wind B consists of *i*) a floor of ≈ 2.8 nT, *ii*) a component ranging from ≈ 0 nT to ≈ 3 nT that varies from cycle to cycle in concert with the solar polar fields (and thus can be used to predict the peak sunspot number of the subsequent maximum), and *iii*) a small/negligible contribution from CMEs (Figure 3).

We equate the floor with a constant open flux of $\approx 8 \times 10^{13}$ Wb. Based on *in-situ* observations since 1972 (Figure 4) and particularly during 2009 (Table 4), at the depth of the current solar minimum, we suggest that, for near-floor conditions, this constant open flux is carried by slow solar wind with speed ≈ 300 km s^{-1}.

The concept of a floor in the solar wind, as developed here, is based on the assumption that the linear relationships in Figures 1 and 2 can be linearly extrapolated beyond the range over which they were derived. The physical implication of this assumption is that the magnetized solar wind persists in the absence (or near absence) of the solar polar fields and the sunspot cycle.

3.2. Update on the Floor

What has changed since Svalgaard and Cliver (2007) introduced the concept of a floor? First, the observations during the present solar minimum from *Ulysses* and near Earth require the floor to be lower than ≈ 4.6 nT. The ≈ 2.8 nT intercept in Figures 1 and 2 easily accommodates these new observations. The ≈ 4 nT floor value deduced by Owens *et al.* (2008) [or the revised value of ≈ 3.7 nT (Crooker and Owens, 2010)] from an analysis of CME rates appears to be too high, because it does not permit the further drop in the solar polar field strength [DM or its proxy, $B_{\rm MIN}$] required to drive the peak SSN lower [to the low values (≈ 10) observed during the Maunder Minimum], in the precursor relationship in Figure 2. In retrospect, the originally proposed floor value of ≈ 4.6 nT had the same problem. If the polar fields and B returned to the same values at each 11-year minimum, there would be no basis for the precursor method of predicting the next $\rm SSN_{MAX}$ and, presumably, no cycle-to-cycle variation of $\rm SSN_{MAX}$. The baseline open flux obtained here of ≈ 1 nT is only one-quarter of the estimate of $\approx 4 \times 10^{14}$ Wb from Svalgaard and Cliver (2007). The difference is due to the reduction in the floor value of B (from ≈ 4.6 nT to ≈ 2.8 nT) and the additional reduction in $B_{\rm R}$ resulting from one-day pre-averaging (Lockwood *et al.*, 2006; Lockwood, Rouillard, and Finch, 2009; Lockwood, Owens, and Rouillard, 2009a, 2009b; Rouillard, Lockwood, and Finch, 2007).

The second major change in the view of the floor presented here from that in Svalgaard and Cliver (2007) involves its origin. In that article it was argued that the floor in B was due to a constant-baseline open flux from both high-speed streams and slow solar wind on which transient flux from sunspot-related activity was superimposed (see also Owens and Crooker, 2006). Here we suggest that it is the SSW alone that is the source of the lower floor in B and the corresponding unvarying component of the open flux. The varying polar field (manifested by HSSs from polar coronal holes) component provides the "seed field" for the next sunspot maximum.

We attribute the drop in $B_{\rm MIN}$ in 2008 and 2009 to values below the superseded ≈ 4.6 nT value of the floor to the $\approx 45\%$ decrease in the solar polar-field strength between the minima preceding Cycles 23 and 24. In contrast, Crooker and Owens (2010) do not take the change in polar fields into account in their explanation of the low $B_{\rm MIN}$ values during 2008 – 2009, but rather suggest that the drop in B is the result of changes in CME properties (slower,

with smaller mass, and originating in weaker-field regions) during the current minimum. Table 1, however, indicates that the average CME contribution to B during 2006 – 2009 (0.22 nT) was comparable to that (0.25 nT) from 1993 – 1996, in comparison with a drop in average B from 5.9 nT to 4.4 nT between these two minimum periods. Crooker and Owens speculate that a higher rate of interchange reconnection during the current minimum may also play a role in producing the low B values in 2008 and 2009. In an alternative view, Zhao and Fisk (2010) use the ratio of O^{7+} to O^{6+} solar-wind ions to distinguish between open flux originating within and outside the streamer-belt "stalk" region. They note that the source region of the slow solar wind from the streamer stalk is narrower during the current solar minimum than it was during the mid-1990s (changing from $\approx 40^{\circ}$ to $15 – 20^{\circ}$), presumably resulting in the observed reduction of open flux. They point out that the open flux outside the streamer stalk was conserved, with the larger area being balanced by a reduced magnetic field. This picture is not consistent with our Figure 4, which shows that the decrease in B between the 1996 and 2009 minima was primarily due to a reduced contribution from high-speed streams, consistent with the decrease in the solar polar-field strength. To sum up this paragraph, the three principal proponents of a floor each point to a different solar wind component (HSSs, CMEs, and SSW) as the cause of the low B values in 2008 – 2009.

As to the origin of the slow flows that we identify with the floor, we note that Judge and Saar (2007) concluded that the radiative and surface magnetic properties of two main sequence "flat activity" stars were similar to those of the Sun at 11-year minima. Such stars are candidates to be in a Maunder Minimum state. Thus Judge and Saar suggested that, "... during the Maunder Minimum, the Sun also had significant small-scale (supergranular and granular) surface magnetic fields..." They continued, "A speculative picture thus emerges of the Sun's Maunder Minimum magnetic field. The small-scale (supergranular) field persisted, but the large-scale (low-order multipolar) structure imposed by sunspot emergence was significantly reduced." The complex coronas observed at solar minima in 1901 and 2009 (Figure 6) are consistent with an increased role for higher-order multipoles (Judge *et al.*, 2010). Given the persistence of the solar wind during the current 11-year minimum [as well as the cosmic-ray modulation cycle during the Maunder Minimum (see, *e.g.*, Berggren *et al.*, 2009)], we hypothesize that these presumably always-present small-scale fields are the source of the slow solar wind and a constant baseline open flux responsible for the inferred floor in B. Borovsky (2008) has argued that the solar wind is composed of a network of magnetic flux tubes which map back to granule and supergranule size scales on the Sun and which carry an amount of flux corresponding to that in field concentrations in the magnetic carpet.

The origin of the slow solar wind is a lively research topic with two principal hypotheses (see the discussion by Riley *et al.*, 2010). In wave-turbulence driven models of the solar wind (Cranmer, van Ballegooijen, and Edgar, 2007), the slow solar wind results from the large expansion factors of open field lines at the boundaries of coronal holes (Wang and Sheeley, 1990). Alternatively, in reconnection/loop-opening (RLO) or stress-heating models of the solar wind (Fisk, 2003; Fisk and Zurbuchen, 2006), the slow solar wind is produced in initially closed regions that open under stress to release plasma. Insofar as coronal holes and high-speed streams appear to vanish (or nearly so) at the floor while slow solar wind seems to dominate at these times, the picture suggested in Figure 4 favors the RLO scenario.

3.3. Update on Long-Term Solar-Wind Reconstructions of B and Φ

During the past few years there has been a remarkable convergence of reconstructions of solar-wind B based on both geomagnetic and cosmogenic-nuclei data for the pre-space-

age years of the 20th century. The controversy (see, *e.g.,* Lockwood, Stamper, and Wild, 1999; Lockwood *et al.*, 2006; Svalgaard and Cliver, 2005, 2006) over the reconstruction of B for this period is now largely resolved (see Figure 12 in Svalgaard and Cliver, 2010). Equation (1), with B_R taken from the regression relationship in Figure 5, shows that between the minimum years of 1901 and 1954, Φ increased from 1.66×10^{14} Wb to 3.05×10^{14} Wb, *i.e.* by 84%, before decreasing to 1.77×10^{14} Wb during 2009.[4] The 84% increase from 1901 – 1954 is in good agreement with that (87%) reported by Rouillard, Lockwood, and Finch (2007). In addition, the Φ decrease by a factor of 1.93 between the 1986 and 2009 minima (Table 1) is comparable to that (factor of 1.98) obtained by Lockwood, Rouillard, and Finch (2009) using the kinematic correction.

A separate disagreement has recently arisen between reconstructions of B based on geomagnetic data and those based on cosmogenic nuclei. In the latest reconstruction of solar wind B based on the ^{10}Be concentration in ice cores, Steinhilber *et al.* (2010) found nine periods during the past 10^4 years where B dropped to zero, violating the notion of a floor. Going back in time, the first of these extreme dips in B is associated with the Spörer Minimum (Eddy, 1976) from $\approx 1420 - 1570$. These deep minima, which stand out on the long-term reconstruction of Steinhilber *et al.* (2010), raise fundamental questions. *i*) Can the solar wind go away? *ii*) Can an unmagnetized solar wind exist? [The correlation found by Schwadron and McComas (2008) between the solar-wind power and the Sun's total open magnetic flux indicates that it cannot.] Investigation of a smaller discrepancy between the ^{10}Be- and geomagnetic-based reconstructions of B for the $\approx 1885 - 1905$ interval could shed light on the nature [or reality (Webber and Higbie, 2010a, 2010b; Webber, Higbie, and Webber, 2010)] of the extreme excursions of B deduced from the ^{10}Be record.

3.4. Observational Tests of the Floor

The existence, or not, of a floor can only be confirmed the extreme occurrence of a return to a Maunder Minimum condition, *i.e.* an extended interval of very low sunspot activity. We may or may not be heading toward such a minimum. The last occurrence of a deep 11-year minimum like that from which we are just emerging was at the beginning of the 20th century. During the current minimum, annual averages of B for 2006 (5.03 nT), 2007 (4.48 nT), 2008 (4.23 nT), and 2009 (3.93 nT) are comparable to those derived from the IDV index (Svalgaard and Cliver, 2010) for 1899 (5.13 nT), 1900 (4.47 nT), 1901 (4.06 nT), and 1902 (4.13 nT) corresponding to the solar minimum preceding Cycle 14. The observed SSN_{MAX} for Cycle 14 (77, corrected following Svalgaard, 2010) is similar to that predicted for Cycle 24 (75 ± 8, Svalgaard, Cliver, and Kamide, 2005; 65 ± 22, this article). Cycle 14 did not presage a return to Maunder Minimum conditions but instead had the smallest SSN_{MAX} during the Gleissberg Minimum of ≈ 100 years ago.

Short of a Maunder-type minimum occurring within the next few solar cycles, we can get an indication about the reality of the floor and the picture of the solar wind during solar-minimum conditions proposed in Figure 3 from the following:

i) the accuracy of the precursor-based prediction for the peak of cycle 24 and subsequent cycles,
ii) the relationship between the solar dipole-field strength and B_{MIN} for the minima preceding cycle 25 and beyond, and

[4] With B for 1901 and 1954 taken from Table 2 and $V = 334$ km s^{-1} for 1901 and 479 km s^{-1} for 1954 deduced from Equation (9) in Svalgaard and Cliver (2007).

iii) the continuation of the quasi-constant contribution of SSW to B during wide excursions in the general level (both 11-year and secular) of solar activity.

Acknowledgements We thank Leif Svalgaard for numerous discussions, Ken Schatten for comments on a draft of this paper, and the referee for helpful criticism. We thank Ian Richardson for providing us with his decomposition of the solar wind into its three principal components. A.G.L. acknowledges support from AFRL contract FA8718-05-C-0036.

References

Balogh, A., Smith, E.J.: 2006, Am. Geophys. Union Fall Meeting, Abstract No. SH44A-05.
Balogh, A., Smith, E.J., Tsurutani, B.T., Southwood, D.J., Forsyth, F.J., Horbury, T.S.: 1995, *Science* **286**, 1007.
Beer, J., Tobias, S., Weiss, N.: 1998, *Solar Phys.* **181**, 237.
Berggren, A.-M., *et al.*: 2009, *Geophys. Res. Lett* **36**, L11801. doi:10.1029/2009GL038004.
Borovsky, J.E.: 2008, *J. Geophys. Res.* **113**, A08110. doi:10.1029/2007JA012684.
Cranmer, S.R., van Ballegooijen, A.A., Edgar, R.J.: 2007, *Astrophys. J. Suppl.* **171**, 520.
Crooker, N.U., Owens, M.J.: 2010, In: Cranmer, S., Hoeksema, T., Kohl, J. (eds.) *Proc. of SOHO 23: Understanding a Peculiar Minimum* **CS-428**, Astron. Soc. Pacific, San Francisco, 279.
Crooker, N.U., Gosling, J.T., Kahler, S.W.: 2002, *J. Geophys. Res.* **107**, 1028. doi:10.1029/2001JA000236.
Eddy, J.A.: 1976, *Science* **192**, 1189.
Fisk, L.A.: 2003, *J. Geophys. Res.* **108**, A41157. doi:10.1029/2002JA009284.
Fisk, L.A., Schwadron, N.A.: 2001, *Astrophys. J.* **560**, 425.
Fisk, L.A., Zurbuchen, T.H.: 2006, *J. Geophys. Res.* **111**, A09115. doi:10.1029/2005JA011575.
Hoyt, D.V., Schatten, K.H.: 1998, *Solar Phys.* **181**, 491.
Judge, P.G., Saar, S.H.: 2007, *Astrophys. J.* **663**, 653.
Judge, P.G., Burkepile, J., de Toma, G., Druckmüller, M.: 2010, In: Cranmer, S., Hoeksema, T., Kohl, J. (eds.) *Proc. of SOHO 23: Understanding a Peculiar Minimum* **CS-428**, Astron. Soc. Pacific, San Francisco, 171.
Livingston, W., Penn, M.: 2009, *Eos, Trans. Am. Geophys. Union* **90**, 257.
Lockwood, M., Owens, M.: 2009, *Astrophys. J.* **701**, 964.
Lockwood, M., Stamper, R., Wild, M.N.: 1999, *Nature* **399**, 437.
Lockwood, M., Rouillard, A.P., Finch, I.D.: 2009, *Astrophys. J.* **700**, 937.
Lockwood, M., Owens, M., Rouillard, A.P.: 2009a, *J. Geophys. Res.* **114**, A11103. doi:10.1029/2009JA014449.
Lockwood, M., Owens, M., Rouillard, A.P.: 2009b, *J. Geophys. Res.* **114**, A11104. doi:10.1029/2009JA014450.
Lockwood, M., Forsyth, R.B., Balogh, A., McComas, D.J.: 2004, *Ann. Geophys.* **22**, 1395.
Lockwood, M., Rouillard, A.P., Finch, I., Stamper, R.: 2006, *J. Geophys. Res.* **111**, A09109. doi:10.1029/2006JA011640.
Owens, M.J., Crooker, N.U.: 2006, *J. Geophys. Res.* **111**, A10104. doi:10.1029/2006JA011641.
Owens, M.J., Crooker, N.U.: 2007, *J. Geophys. Res.* **112**, A06106. doi:10.1029/200gJA012159.
Owens, M.J., *et al.*: 2008, *Geophys. Res. Lett.* **35**, L20108. doi:10.1029/2008GL035813.
Penn, M.J., Livingston, W.: 2006, *Astrophys. J. Lett.* **649**, L45.
Pneuman, G.W., Kopp, R.A.: 1971, *Solar Phys.* **18**, 258.
Richardson, I.G., Cliver, E.W., Cane, H.V.: 2000, *J. Geophys. Res.* **105**, 18 203.
Richardson, I.G., Cane, H.V., Cliver, E.W.: 2002, *J. Geophys. Res.* **107**, 1187. doi:10.1029/2001JA000504.
Riley, P., Mikic, Z., Lionello, R., Linker, J.A., Schwadron, N.A., McComas, D.J.: 2010, *J. Geophys. Res.* **115**, A06104. doi:10.1029/2009JA015131.
Rouillard, A.P., Lockwood, M., Finch, I.: 2007, *J. Geophys. Res.* **112**, A05103. doi:10.1029/2006JA012130.
Schatten, K.H.: 1971, *Cosm. Electrodyn.* **2**, 232.
Schatten, K.H., Scherrer, P.H., Svalgaard, L., Wilcox, J.M.: 1978, *Geophys. Res. Lett.* **5**, 411.
Schwadron, N.A., McComas, D.J.: 2008, *Astrophys. J. Lett.* **686**, L33.
Smith, E.J., Balogh, A.: 1995, *Geophys. Res. Lett.* **22**, 3317.
Smith, E.J., Balogh, A.: 2008, *Geophys. Res. Lett.* **35**, L22103. doi:10.1029/2008GL035345.
Steinhilber, F., Abreu, J.A., Beer, J., McCracken, K.G.: 2010, *J. Geophys. Res.* **115**, A01104. doi:10.1029/2009JA014193.
Svalgaard, L.: 2010, In: Cranmer, S., Hoeksema, T., Kohl, J. (eds.) *Proc. of SOHO 23: Understanding a Peculiar Minimum* **CS-428**, Astron. Soc. Pacific, San Francisco, 297.

Svalgaard, L., Cliver, E.W.: 2005, *J. Geophys. Res.* **110**, A12103. doi:10.1029/2005JA011203.
Svalgaard, L., Cliver, E.W.: 2006, *J. Geophys. Res.* **111**, A09110. doi:10.1029/2006JA011678.
Svalgaard, L., Cliver, E.W.: 2007, *Astrophys. J. Lett.* **661**, L203.
Svalgaard, L., Cliver, E.W.: 2010, *J. Geophys. Res.* **115**, A09111. doi:10.1029/2009JA015069.
Svalgaard, L., Schatten, K.: 2008, Am. Geophys. Union, Fall Meeting, 2008, Abstract#SH51A-1593.
Svalgaard, L., Cliver, E.W., Kamide, Y.: 2005, *Geophys. Res. Lett.* **32**, L01104. doi:10.1029/2004GL021664.
Wang, Y.-M., Sheeley, N.R. Jr.: 1990, *Astrophys. J.* **355**, 726.
Wang, Y.-M., Sheeley, N.R. Jr.: 1994, *J. Geophys. Res.* **99**, 6597.
Wang, Y.-M., Sheeley, N.R. Jr.: 1995, *Astrophys. J. Lett.* **447**, L143.
Wang, Y.-M., Sheeley, N.R. Jr.: 2002, *J. Geophys. Res.* **107**, 1302. doi:10.1029/2001JA000500.
Wang, Y.-M., Sheeley, N.R. Jr.: 2009, *Astrophys. J. Lett.* **649**, L11.
Webber, W.R., Higbie, P.R.: 2010a, *J. Geophys. Res.* **115**, A05102. doi:10.1029/2009JA014532.
Webber, W.R., Higbie, P.R.: 2010b, *J. Geophys. Res.*, arXiv:1003.4989v1 [physics.geo-ph].
Webber, W.R., Higbie, P., Webber, C.W.: 2010, *J. Geophys. Res.*, arXiv:1004.2675v1 [physics.geo-ph].
Zhao, L., Fisk, L.: 2010, In: Cranmer, S., Hoeksema, T., Kohl, J. (eds.) *Proc. of SOHO 23: Understanding a Peculiar Minimum* **CS-428**, Astron. Soc. Pacific, San Francisco, 229.